Residue-resolved monitoring of protein hyperpolarization at sub-second time resolution

Mattia Negroni
University Vienna
Dennis Kurzbach (dennis.kurzbach@univie.ac.at)
University Vienna https://orcid.org/0000-0001-6455-2136

Article

Keywords: Dissolution DNP, biomolecular NMR, time resolution, hyperpolarized water, residue selectivity

Posted Date: August 26th, 2021

DOI: https://doi.org/10.21203/rs.3.rs-830313/v1

Version of Record: A version of this preprint was published at Communications Chemistry on October 22nd, 2021. See the published version at https://doi.org/10.1038/s42004-021-00587-y.

Abstract

We propose a method for real-time nuclear magnetic resonance (NMR) spectroscopy of hyperpolarized proteins at residue resolution. The approach is based on dissolution dynamic nuclear polarization (*d*-DNP), which enables the use of hyperpolarized buffers that selectively boost NMR signals of backbone amides that incur magnetization fast from their surroundings. Capitalizing on the resulting spectral sparseness and simultaneous signal enhancement, we obtained residue-resolved NMR spectra at a sampling rate of 2 Hz. We could thus track the evolution of hyperpolarization at different protein residues simultaneously with time. This was achieved under near-physiological conditions, *i.e.*, in aqueous solution at physiological salt concentration and at 37° C. With this development, two often encountered limitations of conventional solution-state NMR can be addressed: 1) NMR experiments are typically performed under conditions that increase sensitivity but are physiologically not relevant (low pH, low temperature) and; 2) signal accumulation over long periods impedes the determination of fast (on the order of seconds) real-time monitoring. Both limitations are of equal fundamental relevance: interaction studies under non-native conditions are of limited pharmacological relevance, and the key to the function of proteins often resides in their interaction kinetics. The proposed technique possibly opens new routes towards residue and temporally resolved spectroscopy at the atomistic level by overcoming the need for signal averaging in residue-resolved protein biomolecular NMR.

Background

Processes involving protein interactions such as enzymatic reactions,[1-2] biomineralization[3-4], or molecular recognitions[5-6] evolve in time towards an equilibrium state. However, it is notoriously challenging to access this temporal dimension while simultaneously maintaining high structural resolution.[6-9] This is not least because nuclear magnetic resonance (NMR) spectroscopy, the central method to access protein structures in solution, typically focuses on systems in chemical equilibrium.[10-11] This limitation is imposed by weak signal intensities that necessitate longer signal averaging periods and thus impede time-resolved studies. However, to adequately describe processes that evolve over time, methods are required that improve NMR signal intensities and, at the same time, capitalize on the method's intrinsically high (atomistic) resolution. We here propose such a method based on dissolution dynamic nuclear polarization-boosted NMR and spin hyperpolarization.[12-14]

Indeed, hyperpolarization, in particular dissolution dynamic nuclear polarization (*d*-DNP) has recently been developed to enhance NMR signals in residue-resolved studies of proteins[15-20] and nucleic acids[21] at substantially improved signal intensities. To this methodological portfolio, we add a time aspect.

Due to the implementation of *d*-DNP as an 'ex-situ' technique, with an external hyperpolarization setup, it is applicable to almost any type of molecule in solution. It provides up to >10.000-fold enhanced signal intensities. As a result, this method enables access to time-resolved NMR data on milliseconds to seconds timescales while guaranteeing applicability to a broad spectrum of target molecules. However, d-DNP has not yet found many applications in biomolecular NMR despite these exceptional benefits. This is not least since one has to give up the major advantage of solution-state protein NMR, namely residue-resolution. Indeed, the

latter stimulated a large share of the timely NMR developments, including the development of a 1.2 GHz NMR spectrometer.[22]

Here we present a novel strategy that aims to overcome this predicament by using hyperpolarized water to enhance nuclear magnetic resonance proton signals in proteins. Owing to this signal boost, we were able to achieve simultaneously time- and residue-resolved NMR spectra of proteins.

This development addresses two major limitations of conventional solution-state NMR: 1) Experiments are often performed under conditions that increase sensitivity but are physiologically not relevant (low pH, low temperature) and; 2) signal accumulation over long periods impedes the determination of fast (on the order of milliseconds to seconds) real-time monitoring. Both limitations are of equal fundamental relevance: interaction studies under non-native conditions are of limited pharmacological relevance, and the key to the function of proteins often resides in their interaction kinetics.

Methods

Our experimental strategy is based on two key concepts: hyperpolarized buffers and selective detection.

(*1*) *Hyperpolarized sample buffers*.[23-24] These can be used to enhance the signals in protein NMR. Hyperpolarization is here understood as a non-equilibrium state where the nuclear spins constructively align along the magnetic field B_0 to yield stronger signal amplitudes. This signal boost can be transferred from a hyperpolarized solvent to a protein of interest through chemical exchange and NOE effects.[25-26] With such techniques, substantial signal enhancements of several orders of magnitude can be achieved.

(*2*) *Selective detection*.[17, 25] It is possible to select a small subset of hyperpolarized residues for detection using tailored NMR pulse sequences. As will be shown, spectra can be rendered so sparse that real-time monitoring at high sampling rates of individual amino acids becomes possible if boosted by hyperpolarization.

In the following, these two concepts are going to be outlined first. Then, we demonstrate how to combine them to achieve hyperpolarized real-time NMR of proteins.

(*i*) Dissolution dynamic nuclear polarization as a tool to enhance protein signals

The experimental strategy for signal amplification of proteins via hyperpolarized buffers has been laid out in a series of recent publications.[15-18, 25, 27-28] The method is based on the dissolution dynamic nuclear polarization (*d*-DNP) technique. The procedure generally consists of three steps (Fig. 1):

(1) preparation of hyperpolarized, *i.e.* NMR-signal amplified water protons by DNP at cryogenic temperatures (here T_{DNP} = 1.2 K) and high magnetic field (here $B_{0,DNP}$ = 6.7 T) achieved by off-resonance microwave irradiation (here ν_{DNP} = 188.38 GHz).

(2) After the build-up, the hyperpolarized H_2O is dissolved with a burst of superheated D_2O and rapidly (here $t_{transfer}$ = 1.5 s) injected into an NMR tube waiting in a high-field detection spectrometer (here $B_{0,NMR}$ = 18.8 T,

T_{NMR} = 310 K), where it mixed *in-situ* with a solution of the target protein. After completion of the mixing process, NMR detection is triggered. Here we acquired time series of $^{1}H^{N}$-selective ^{15}N-edited 1D ^{1}H spectra (similar to the first transient in a BEST-HMQC experiment)[29] for 50 s after mixing. The pulse sequence was applied without any water suppression in order to not accelerate the depletion of the hyperpolarized pool of protons (see the Supporting Information for details).[29]

(3) During the detection period, proton chemical and magnetic (*i.e.,* nuclear Overhauser effects; NOE) exchange processes between the buffer and the target protein introduce ^{1}H-hyperpolarization into the latter, thereby selectively enhancing NMR signals of residues with favorable solvent interactions.[25-26]

The resulting signal enhancement that can be achieved is exemplified in Fig. 1 (right) for the model protein Ubiquitin (Ubq) under near-physiological conditions, *i.e.*, in aqueous solution at physiological salt concentrations, at pH 7.4 and 37 °C. Boosted signal amplitudes can be observed directly after mixing with hyperpolarized water. With time, the signal amplitudes decay since the spin hyperpolarization relaxes towards thermal equilibrium. Many resonances even drop below the detection threshold after the signal boost has decayed. The physiological buffer conditions accelerate amide proton exchange and thus do not yield good signal intensities in non-hyperpolarized spin systems.

(*ii*) Selecting a set of residues for detection

The hyperpolarization exchange efficiency during step (3) of the *d*-DNP procedure depends on various factors.[17, 25-26] For a given buffer and temperature, the most important factors are the delay d_1 between successive NMR detections as well as the structure of the target protein, which determines solvent exposure, as well as chemical exchange and NOE rates. We exploit this feature by fine-tuning d_1 such that only a subset of residues with strong solvent interaction becomes sufficiently hyperpolarized for single-scan NMR detection.

Table 1. Enhancement factors and apparent decay rates of the 10 fitted lines.

Residue	L8	A46	Q2	T14	L71/T12/Q49/R42	D39/I23	R74	L69	n/a	G47
e	2.7	2.2	>11.6	6.2	12.4	9.1	12.8	5.0	>11.6	3.4
$R_{1,app}$ / s^{-1}	0.14	0.29	0.25	0.7	0.15	0.16	0.16	0.13	0.19	0.11

To explore and put this dependency to use, we employed water-selective nuclear Overhauser spectroscopy (WS-NOESY; Fig. 2a). Its three functional elements are: (a) A presaturation pulse-sequence that deletes all protein polarization, *i.e.,* protein NMR signals, (b) a mixing period τ_m during which polarization from the hyperpolarized buffer can be transferred to the protein and (c) a 2D ^{1}H-^{15}N (HSQC) sequence for detection. This design allows quantification of the transferred polarization from the solvent to the protein at residue resolution. The WS-NOESY approach to determine polarization transfer has been used in a series of recent publications by Kadeřávek et al.[25] and Hilty and co-workers.[16, 28] They showed that proton exchange between

water and protein transfers polarization to the latter depending on residue-specific exchange rates and exchange-relayed NOEs.

Here we add time-traces of polarization exchange to the current picture. In particular, we investigate the dependence on the mixing time τ_m. In line with our earlier work[25], this confirmed that the transfer kinetics critically depends on the efficiency of solvent interaction of a residue. Fig. 2b displays the signal $^1H^N$ build-up due to the polarization transfer for our experimental conditions at the example of two residues, for slow (Q2, left panel) and fast (L8, right panel) transfer (data for all other residues can be found in the Supporting Information). The build-up curves show how the polarization is transferred from the solvent to the protein. The signal intensity for mixing times of 500 ms are indicated (corresponding to the interscan delay in *d*-DNP experiments, *vide infra*). For residue Q2 only little polarization is replenished within this time, while the opposite holds for L8.[30]

Impact on hyperpolarization efficiency

For a protein in a hyperpolarized buffer, the kinetics of polarization transfer determines the hyperpolarization efficiency. In a *d*-DNP experiment, the mixing time corresponds to the delay between successive detections during which protein polarization is replenished. This is confirmed in Fig. 2c, which shows residue-resolved signal intensities found in WS-NOESY at τ_m = 0.5 s together with yellow bars that indicate residues observed in *d*-DNP experiments for an interscan delay of 0.5 s (cf. Fig. 3). The evident correspondence between both experiments demonstrates that proton exchange and weak NOE can account for site-specific protein signal enhancement in hyperpolarized buffers.[25] We capitalize on this effect as it enables selective enhancement of a sub-set of residues of a globular protein in a *d*-DNP experiment by exploiting the elimination of residue signals with slow polarization-exchange kinetics at short mixing times.

(*iii*) Residue and temporally resolved real-time NMR of proteins

Signal suppression at short mixing times can be used to achieve real-time monitoring of hyperpolarized Ubq at residue resolution. Choosing $\tau_m \approx 0.5$ s, the spectra become so sparse that only 13 signals can be observed in the WS-NOESY experiments. Thus, it is possible to deconvolute the signals of individual residues even in one-dimensional NMR. The correspondence between the signals observed in a WS-NOESY at a τ_m of 0.5 s and the observed signals in a ^{15}N-edited ^{1}H 1D spectrum is shown in Fig. 3a. The 13 2D cross-peaks project onto 10 discernible lines in the 1D spectrum. This allows the assignment of most resonances in the latter. Indeed, 7 residues can unambiguously be identified (see Table 1). Due to this, the following experiment was possible:

Hyperpolarized water was first mixed with a Ubiquitin solution. After mixing, a series of ^{15}N-edited ^{1}H spectra were recorded with an interscan delay of 0.5 s (according to τ_m in the sparse WS-NOESY).

Fig. 3b shows a selection of 1D spectra from this time series and corresponding fits of 10 Lorentzians to the spectrum. Due to the spectral sparseness, the signals become deconvolutable, and it is possible to follow the hyperpolarization level of individual residues in real-time. The determined residue-resolved signal enhancements are mapped onto the structure of Ubq in Fig. 3c. The corresponding time-dependent signal

intensities are displayed in Fig. 3d. The figure shows how the signals are enhanced after mixing due to the exchange of hyperpolarization (at t=0). With time the polarization decays towards thermal equilibrium.

The observed decay rates are functions of the water proton and $^{1}H^{N}$ relaxation rates as well as of the proton exchange rate and detection pulse angles as shown by Szekely et al.[17] Since the first two factors are residue dependent varying apparent hyperpolarization decay rates can be observed for individual residues. Qualitatively, we observe that residues buried in the hydrophobic regions of the protein show faster relaxation due to less efficient replenishment of hyperpolarized protons, while residues in flexible regions show slower apparent decays (*e.g.,* residue 14: 0.7 s^{-1} *vs*. residue 47: 0.11 s^{-1}; cf. Table 1). Generally, the decay rates are low enough to detect boosted signals for 20 s after mixing the protein and the hyperpolarized buffer.

It should be noted that the relationships between signal enhancement, type of residue, and contributions of NOE effects in Ubiquitin have been discussed in detail by Kadeřávek et al. (see reference [25]). It was found that solvent-relayed NOEs contribute to enhancing a small subset of residues (including D39, Q49, and K63) that feature protic side chain moieties, thereby boosting the signal intensity even further. This is also in line with the finding that residues with high enhancements here (see Table 1) feature such side chains. Yet, Kadeřávek et al.[25] also found that the major contribution to the signal enhancement is due to chemical proton exchange in fast exchanging residues localized in loop 1 and b sheet 2.

Experimental

Protein expression All protein samples were expressed and purified following the protocol published earlier.[25] The protein was provided at a concentration of 1 mM in physiological saline at pH 7.4 and 37˚C.

Dissolution DNP: 180 mL of a 15 mM TEMPOL solution in a 0.85:0.15 v/v/v mixture of H_2O and glycerol was vitrified in liquid helium. The glassy sample was positively hyperpolarized at 1.2 K in a magnetic field of 6.7 T by partial saturation of the EPR spectrum at 187.7 GHz (Bruker Biospin, ENS Paris). Under these conditions, the hyperpolarization build-up rates were found to be $R_{build\text{-}up}$ = (4.8 ± 0.1) 10^{-5} s^{-1}. Hence hyperpolarization build-up times of 3h were used. Dissolution was achieved with a burst of 5 mL D_2O at 180 °C (453 K) under 1.05 MPa. The sample was subsequently propelled to a detection NMR spectrometer operating at 18.8 T (800 MHz for ^{1}H) and 37 °C (310 K) within 1.5 s with He gas under 0.7 MPa through a “magnetic tunnel”[33] maintaining a constant magnetic field of 0.9 T over a distance of approximately 4 m. The delay for mixing with the target protein solution (150 mL) and settling of turbulence prior to initiation of the NMR experiments was 3 s. After dissolution, the H_2O:D_2O ratio was 1:0.03.

For detection, the pulse sequence shown in Fig. S4 was used. For the ^{1}H channel, a selective 1000 ms long PC90 pulse was used for 90° excitation, and a 2000 ms long REBURP pulse was used for inversion. The carrier frequency was set to 10 ppm to avoid pulsing on the water resonance. Hence, only signals with chemical shifts >8 ppm were detected. Single scan detection was used, no phase cycling was applied. All data was apodized prior to Fourier transformation using a Guassian window function. For detecting the ^{15}N-edited ^{1}H-1D time series, a selective 1000 ms long PC90 pulse was used for 90° excitation, and a 2000 ms long REBURP pulse was used for inversion on the ^{1}H channel. The carrier frequency was set to 10 ppm to avoid

pulsing on the water resonance. The rectangular shapes indicated 90˚pulses. Hence, only signals with chemical shifts >8 ppm were detected. d2 was set to 0.00345 s, d1 to 0.5 s, and d0 to 0.00002780 s. d0 was not incremented. The FID was detected for 0.1 s during GARP decoupling

The data were fitted with Lorentzian functions by adapting an approach outlined earlier in references [9, 34].

NMR spectroscopy For the ^{1}H-^{15}N WS-NOESY experiments the pulse sequence of Fig. 2a was used.

The presaturation block selectively saturates all non-water protons of the system with a p/2 - z-gradient - p - z-gradient - p/2 sequence. For the water-selective p pulse, a 7.5 ms long Gaussian-shaped pulse was used with a carrier frequency centered at 4.7 ppm. The ^{15}N pulses were centered at 118.5 ppm. During the mixing delay, the 180° pulse compensates for relaxation effects, and the weak gradients suppress radiation damping. The HSQC block is a conventional gradient-selective pulse sequence using the 3-9-19 Watergate for solvent suppression. All spectra were recorded on a Bruker NEO spectrometer operating at a proton Larmor frequency of 600 MHz. The spectrometer was equipped with a prodigy TCI probe. The p/2 pulse length was 11.1 ms for the ^{1}H channel and 37 ms for the ^{15}N channel. The temperature was set to 298 K. 10% D_2O was used as lock solvent in an otherwise physiological saline at pH 7.4. In total, 128 complex increments were detected in the indirect dimension. All data were apodized with a 60 degree shifted sine-bell functions and zero-filled prior to Fourier transformation to twice the FID length. Subsequently, data were baseline corrected along the directly detected dimension using NMR Pipe.[35]

Conclusions

Concluding, with the proposed technique, one can monitor hyperpolarized proteins at residue and high-temporal resolution to track individual diagnostic peaks, reminiscent of selective labeling strategies.

Various applications ranging from determining structural dynamics to drug discovery have significantly profited from such experimental strategies (see, e.g., references [31-32]). Here we aim to capitalize on a similar approach to sparsify protein spectra.

The proposed technique might not be applicable for intrinsically disordered proteins with narrow chemical shift dispersions in the proton dimension. Indeed, earlier work showed that for such proteins 2D or 3D detection is necessary to achieve residue-resolution, albeit lacking time resolution. However, ca. >70% of the proteome are well-folded, and, therefore, the presented technique is applicable to the largest share of target proteins. This approach might thus attract widespread interest as the technique is applicable to a large share of NMR studies.

We want to stress that the presented technique should not be considered as an alternative to established solution-state techniques but instead, as a complementary approach that can be put to use when protein real-time monitoring at residue-resolution is required. We anticipate using this method in, *e.g.,* time-resolved ligand-protein binding studies by mixing the target protein with a hyperpolarized solution of a binding partner. Indeed, most ligand interaction sites (e.g., binding pockets in drug design applications) or catalytically active sites remain incorporated in folded regions, where the presented approach is applicable. In such cases, the proton

pool can boost signal intensities while the binding event proceeds. Indeed, real-time data can be obtained on a millisecond to seconds time scale, which is often impossible to obtain by NMR spectroscopy in thermal equilibrium.

Declarations

Acknowledgments

The project leading to this application received funding from the European Research Council (ERC) under the European Union's Horizon 2020 research and innovation programme (grant agreement 801936). This project was supported by the Austrian FWF (stand-alone grant no. P-33338). The authors thank Dr. Pavel Kadeřávek and Dr. Gregory L. Olsen for helpful discussions.

Conflict of Interest

The authors declare no conflict of interest.

References

1. Sweetlove, L. J.; Fernie, A. R., The role of dynamic enzyme assemblies and substrate channelling in metabolic regulation. *Nat Commun* **2018**, *9* (1), 2136.
2. Holdgate, G. A.; Meek, T. D.; Grimley, R. L., Mechanistic enzymology in drug discovery: a fresh perspective. *Nat Rev Drug Discov* **2018**, *17* (2), 115–132.
3. Gebauer, D.; Wolf, S. E., Designing Solid Materials from Their Solute State: A Shift in Paradigms toward a Holistic Approach in Functional Materials Chemistry. *J Am Chem Soc* **2019**, *141* (11), 4490–4504.
4. Wang, Y.; Azais, T.; Robin, M.; Vallee, A.; Catania, C.; Legriel, P.; Pehau-Arnaudet, G.; Babonneau, F.; Giraud-Guille, M. M.; Nassif, N., The predominant role of collagen in the nucleation, growth, structure and orientation of bone apatite. *Nat Mater* 2012, *11* (8), 724–33.
5. Boehr, D. D.; Nussinov, R.; Wright, P. E., The role of dynamic conformational ensembles in biomolecular recognition. *Nat Chem Biol* **2009**, *5* (11), 789–96.
6. Lee, M. K.; Gal, M.; Frydman, L.; Varani, G., Real-time multidimensional NMR follows RNA folding with second resolution. *Proc Natl Acad Sci U S A* 2010, *107* (20), 9192–7.
7. Gal, M.; Mishkovsky, M.; Frydman, L., Real-time monitoring of chemical transformations by ultrafast 2D NMR spectroscopy. *Journal of the American Chemical Society* 2006, *128* (3), 951–956.
8. Dass, R.; Kozminski, W.; Kazimierczuk, K., Analysis of complex reacting mixtures by time-resolved 2D NMR. *Anal Chem* **2015**, *87* (2), 1337–43.
9. Miclet, E.; Abergel, D.; Bornet, A.; Milani, J.; Jannin, S.; Bodenhausen, G., Toward Quantitative Measurements of Enzyme Kinetics by Dissolution Dynamic Nuclear Polarization. *J Phys Chem Lett* **2014**, *5* (19), 3290–5.
10. Felli, I. C.; Brutscher, B., Recent advances in solution NMR: fast methods and heteronuclear direct detection. *Chemphyschem* **2009**, *10* (9–10), 1356–68.

11. Rule, G. S.; Hitchens, T. K., *Fundamentals of Protein NMR Spectroscopy*. Springer: Dordrecht, 2006.
12. Ardenkjaer-Larsen, J. H.; Fridlund, B.; Gram, A.; Hansson, G.; Hansson, L.; Lerche, M. H.; Servin, R.; Thaning, M.; Golman, K., Increase in signal-to-noise ratio of > 10,000 times in liquid-state NMR. *Proc Natl Acad Sci U S A* 2003, *100* (18), 10158–63.
13. Jannin, S.; Dumez, J. N.; Giraudeau, P.; Kurzbach, D., Application and methodology of dissolution dynamic nuclear polarization in physical, chemical and biological contexts. *J Magn Reson* 2019, *305*, 41–50.
14. Kouřil, K.; Kouřilová, H.; Levitt, M. H.; Meier, B., Dissolution-Dynamic Nuclear Polarization with Rapid Transfer of a Polarized Solid. *Nat Commun* 2019, *10*, 1733.
15. Kurzbach, D.; Canet, E.; Flamm, A. G.; Jhajharia, A.; Weber, E. M.; Konrat, R.; Bodenhausen, G., Investigation of Intrinsically Disordered Proteins through Exchange with Hyperpolarized Water. *Angew Chem Int Ed Engl* **2017**, *56* (1), 389–392.
16. Kim, J.; Liu, M.; Hilty, C., Modeling of Polarization Transfer Kinetics in Protein Hydration Using Hyperpolarized Water. *J Phys Chem B* **2017**, *121* (27), 6492–6498.
17. Szekely, O.; Olsen, G. L.; Felli, I. C.; Frydman, L., High-resolution 2D NMR of disordered proteins enhanced by hyperpolarized water. *Anal Chem* 2018.
18. Sadet, A.; Stavarache, C.; Bacalum, M.; Radu, M.; Bodenhausen, G.; Kurzbach, D.; Vasos, P. R., Hyperpolarized water enhances two-dimensional proton NMR correlations: a new approach for molecular interactions. *J. Am. Chem. Soc.* 2019, *141*, 12448–12452.
19. Olsen, G.; Markhasin, E.; Szekely, O.; Bretschneider, C.; Frydman, L., Optimizing water hyperpolarization and dissolution for sensitivity-enhanced 2D biomolecular NMR. *J Magn Reson* 2016, *264*, 49–58.
20. Ragavan, M.; Iconaru, L. I.; Park, C. G.; Kriwacki, R. W.; Hilty, C., Real-Time Analysis of Folding upon Binding of a Disordered Protein by Using Dissolution DNP NMR Spectroscopy. *Angew Chem Int Ed Engl* **2017**, *56* (25), 7070–7073.
21. Novakovic, M.; Olsen, G. L.; Pinter, G.; Hymon, D.; Furtig, B.; Schwalbe, H.; Frydman, L., A 300-fold enhancement of imino nucleic acid resonances by hyperpolarized water provides a new window for probing RNA refolding by 1D and 2D NMR. *Proc Natl Acad Sci U S A* 2020, *117* (5), 2449–2455.
22. Luchinat, E.; Barbieri, L.; Cremonini, M.; Banci, L., Protein in-cell NMR spectroscopy at 1.2 GHz. *J Biomol Nmr* 2021, *75* (2–3), 97–107.
23. Lipso, K. W.; Bowen, S.; Rybalko, O.; Ardenkjaer-Larsen, J. H., Large dose hyperpolarized water with dissolution-DNP at high magnetic field. *J Magn Reson* 2017, *274*, 65–72.
24. Kouno, H.; Orihashi, K.; Nishimura, K.; Kawashima, Y.; Tateishi, K.; Uesaka, T.; Kimizuka, N.; Yanai, N., Triplet dynamic nuclear polarization of crystalline ice using water-soluble polarizing agents. *Chem Commun (Camb)* 2020, *56* (26), 3717–3720.
25. Kaderavek, P.; Ferrage, F.; Bodenhausen, G.; Kurzbach, D., High-Resolution NMR of Folded Proteins in Hyperpolarized Physiological Solvents. *Chem. Eur. J.* 2018, *24*, 13418–13423.
26. Szekely, O.; Olsen, G. L.; Novakovic, M.; Rosenzweig, R.; Frydman, L., Assessing Site-Specific Enhancements Imparted by Hyperpolarized Water in Folded and Unfolded Proteins by 2D HMQC NMR. *J Am Chem Soc* **2020**, *142* (20), 9267–9284.

27. Olsen, G. L.; Szekely, O.; Mateos, B.; Kaderavek, P.; Ferrage, F.; Konrat, R.; Pierattelli, R.; Felli, I. C.; Bodenhausen, G.; Kurzbach, D.; Frydman, L., Sensitivity-enhanced three-dimensional and carbon-detected two-dimensional NMR of proteins using hyperpolarized water. *J Biomol Nmr* 2020, *74* (2–3), 161–171.
28. Kim, J.; Mandal, R.; Hilty, C., Observation of Fast Two-Dimensional NMR Spectra during Protein Folding Using Polarization Transfer from Hyperpolarized Water. *J Phys Chem Lett* **2019**, *10* (18), 5463–5467.
29. Schanda, P.; Kupce, E.; Brutscher, B., SOFAST-HMQC experiments for recording two-dimensional heteronuclear correlation spectra of proteins within a few seconds. *J Biomol Nmr* 2005, *33* (4), 199–211.
30. Honegger, P.; Steinhauser, O., The protein-water nuclear Overhauser effect (NOE) as an indirect microscope for molecular surface mapping of interaction patterns. *Phys Chem Chem Phys* **2019**, *22* (1), 212–222.
31. Tugarinov, V.; Kanelis, V.; Kay, L. E., Isotope labeling strategies for the study of high-molecular-weight proteins by solution NMR spectroscopy. *Nature Protocols* 2006, *1* (2), 749–754.
32. Pellecchia, M.; Sem, D. S.; Wuthrich, K., NMR in drug discovery. *Nat Rev Drug Discov* **2002**, *1* (3), 211–9.
33. Milani, J.; Vuichoud, B.; Bornet, A.; Mieville, P.; Mottier, R.; Jannin, S.; Bodenhausen, G., A magnetic tunnel to shelter hyperpolarized fluids. *Rev Sci Instrum* **2015**, *86* (2).
34. Kress, T.; Walrant, A.; Bodenhausen, G.; Kurzbach, D., Long-Lived States in Hyperpolarized Deuterated Methyl Groups Reveal Weak Binding of Small Molecules to Proteins. *Journal of Physical Chemistry Letters* **2019**, *10* (7), 1523–1529.
35. Delaglio, F.; Grzesiek, S.; Vuister, G. W.; Zhu, G.; Pfeifer, J.; Bax, A., Nmrpipe - a Multidimensional Spectral Processing System Based on Unix Pipes. *J Biomol Nmr* 1995, *6* (3), 277–293.

Figures

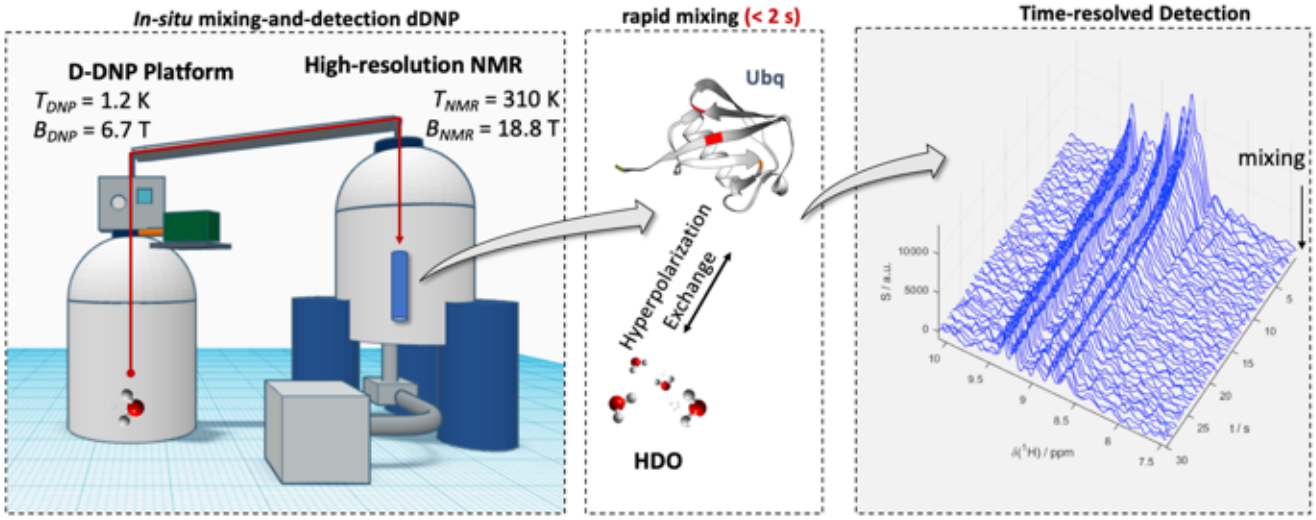

Figure 1

Experimental strategy for real-time hyperpolarized protein NMR. Water is hyperpolarized at TDNP of 1.2 K before it is dissolved and mixed with a Ubq solution waiting at TNMR of 310 K in the NMR spectrometer. After mixing, hyperpolarization is introduced into the protein by chemical and magnetic exchange. Hence, a time

series of NMR spectra can be recorded with superior signal intensities. The right panel shows how the signal intensities of the protein are boosted before the water polarization returns to thermal equilibrium.

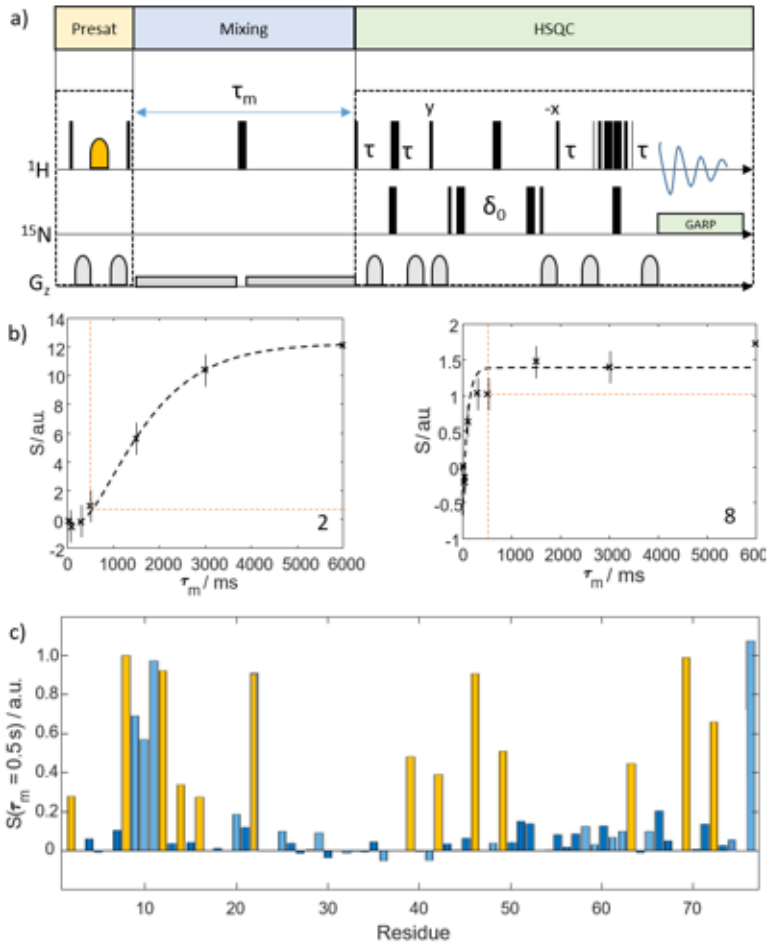

Figure 2

a) WS-NOESY pulse sequence used to measure the efficiency of the polarization transfer from water to the target protein. Thin black bars indicate 90˚ and thick bars 180˚ pulses. The yellow shape indicates a water-selective 180˚ pulse. In the first segment, the protein polarization is deleted. Next, during a mixing delay tm, polarization can be transferred from the water to the protein. Finally, the polarization is read out by means of a 1H-15N Fast-HSQC spectrum. Thus, the by varying tm, the kinetics of the polarization transfer can be assessed. The long weak gradients were used for radiation damping suppression. More details can be found in the Experimental section. b) Experimental time traces (signal intensity S vs. mixing time tm) for residues 2 and 8 showing signal build-up due to magnetic and chemical exchange with the water pool. The differences in build-up kinetics, which we put to use here, are evident. The signal intensity for a mixing time of 0.5 s is indicated by the dashed orange line. Data for all other residues are shown in the Supporting Information c) Residue-resolved signal intensities S for a mixing time of 0.5 s. The yellow bars indicate the residues that where observed in the d-DNP experiments (see main text). The light blue bars indicate residues with resonance frequencies outside the excitation bandwidth in the d-DNP experiments.

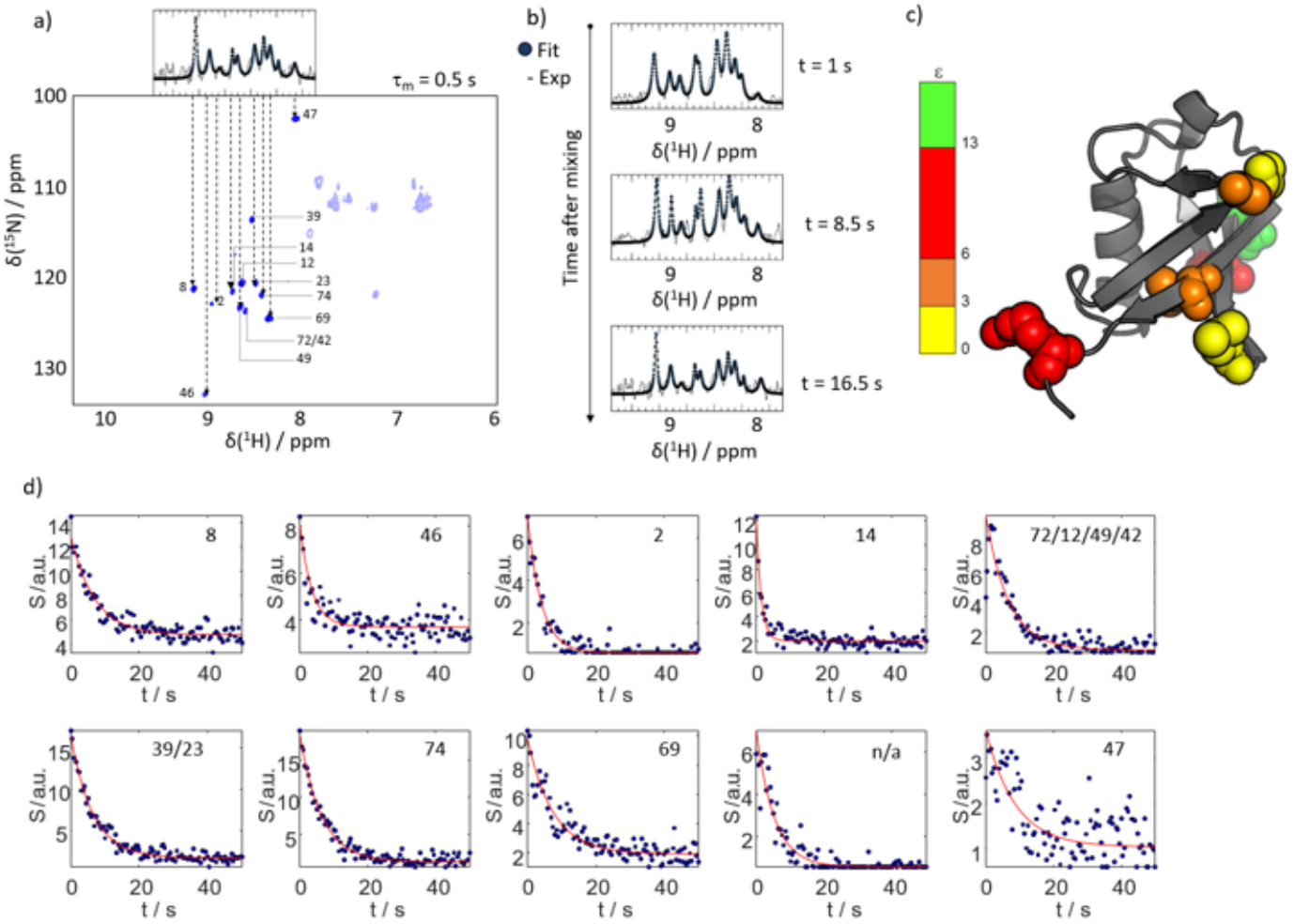

Figure 3

Real-time monitoring of hyperpolarization. a) With an interscan delay of 0.5 s only 10 lines can be detected in hyperpolarized water as shown in the top insert (spectrum as black line, fit to 10 Lorentzians as blue dots). A water-selective NOESY spectra with a mixing time of tm = 0.5 s confirms that only few residues are detectable. For most amino acids and polarization exchange and relaxation effects exactly cancel. Due the sparseness of the spectra most signals in the one-dimensional spectrum can be assigned. The transparent peaks fall out of the detected bandwidth in the d-DNP experiment due to the employed selective amide proton pulses. b) 15N-edited proton 1D spectra of the 10 observable HN protons for different times after mixing with hyperpolarized water (using an interscan delay of 0.5 s; Spectrum as black line, fit to 10 Lorentzians as blue dots). c) Signal enhancements found for the observable residues mapped on the structure of Ubq. d) Time traces of signal intensities for residues the observable lines in the d-DNP experiments. The hyperpolarization decay rates are indicated. The residue indices are indicated. Two lines could not unambiguously be assigned. Another line could not be assigned as no corresponding signal was found in the WS-NOESY (labelled ‘n/a’).

Supplementary Files

This is a list of supplementary files associated with this preprint. Click to download.

- RealtimeNMRatresidueresolutionSI.docx